1-15-2017

Endothelium in the pharyngeal arches 3, 4 and 6 is derived from the second heart field.

Xia Wang
Thomas Jefferson University

Dongying Chen
Thomas Jefferson University

Kelley Chen
Thomas Jefferson University

Ali Jubran
Thomas Jefferson University

AnnJosette Ramirez
Thomas Jefferson University

Authors
Xia Wang, Dongying Chen, Kelley Chen, Ali Jubran, AnnJosette Ramirez, and Sophie Astrof

HHS Public Access

Author manuscript

Dev Biol. Author manuscript; available in PMC 2018 January 15.

Published in final edited form as:

Dev Biol. 2017 January 15; 421(2): 108–117. doi:10.1016/j.ydbio.2016.12.010.

Endothelium in the pharyngeal arches 3, 4 and 6 is derived from the second heart field

Xia Wang[a,1], **Dongying Chen**[b,1,2], **Kelley Chen**[c,1], **Ali Jubran**[d,3], **AnnJosette Ramirez**[b,3], and **Sophie Astrof**[b,*]

[a]Thomas Jefferson University, Department of Medicine, Center for Translational Medicine, 1020 Locust Street, Philadelphia, PA, 19107, USA

[b]Graduate Program in Cell & Developmental Biology, Thomas Jefferson University, Philadelphia, PA

[c]Jefferson Medical College of Thomas Jefferson University, Clinical & Translational Research Track, Philadelphia, PA

[d]The Masters of Science Program in Cell & Developmental Biology, Thomas Jefferson University, Philadelphia, PA

Abstract

Oxygenated blood from the heart is directed into the systemic circulation through the aortic arch arteries (AAAs). The AAAs arise by remodeling of three symmetrical pairs of pharyngeal arch arteries (PAAs), which connect the heart with the paired dorsal aortae at mid-gestation. Aberrant PAA formation results in defects frequently observed in patients with lethal congenital heart disease. How the PAAs form in mammals is not understood. The work presented in this manuscript shows that the second heart field (SHF) is the major source of progenitors giving rise to the endothelium of the pharyngeal arches 3 – 6, while the endothelium in the pharyngeal arches 1 and 2 is derived from a different source. During the formation of the PAAs 3 – 6, endothelial progenitors in the SHF extend cellular processes toward the pharyngeal endoderm, migrate from the SHF and assemble into a uniform vascular plexus. This plexus then undergoes remodeling, whereby plexus endothelial cells coalesce into a large PAA in each pharyngeal arch. Taken together, our studies establish a platform for investigating cellular and molecular mechanisms regulating PAA formation and alteration that lead to disease.

Graphical Abstract

[*]Author for correspondence: Sophie Astrof, Ph.D. Tel.: 617-429-8295; fax: 215-955-1690. sophie.astrof@jefferson.edu.

[1]Co-first authors

[2]Current address: Yale Cardiovascular Research Center, Department of Internal Medicine, Yale University School of Medicine, New Haven, CT 06511, USA

[3]Co-second authors

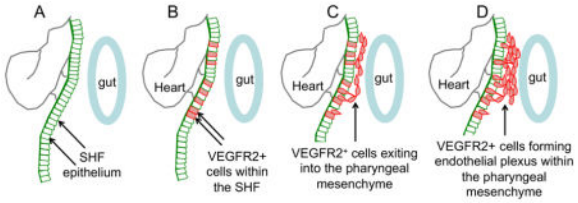

1.0 INTRODUCTION

During embryogenesis, paired pharyngeal arch arteries (PAAs) form symmetrically relative to the embryonic midline, connecting the heart with the dorsal aortae. In birds and mammals, the first and second PAAs regress, whereas the PAAs 3, 4 and 6 undergo asymmetric remodeling giving rise to the aortic arch arteries (AAAs) (Hutson and Kirby, 2007; Olson, 2002). Defects in PAA development are common features of congenital heart disease, warranting further detailed investigation into cellular and molecular mechanisms regulating their formation.

The argument of whether or not mammalian PAAs arise by angiogenesis or by vasculogenesis dates back to the early 1900s (Congdon, 1922). Investigations of human, rabbit, chicken and mouse embryos demonstrated the presence of endothelial plexus in the pharyngeal region prior to the appearance of PAA lumens, and it was hypothesized that this vascular plexus gave rise to the PAAs (Bremer, 1912; Congdon, 1922; DeRuiter et al., 1993a; DeRuiter et al., 1993b; DeRuiter et al., 1992; Li et al., 2012; Waldo et al., 1996). However, the origin of the endothelial cells in the plexus and subsequently, in the PAAs has remained unknown. Resin filling of embryonic vasculature demonstrated the presence of small vascular branches connected to the dorsal aortae and the aortic sac at early stages of PAA formation, suggesting that the PAA endothelium arose by branching off from these vessels (Hiruma et al., 2002). In contrast, recent studies using genetic labeling and the Tie2-Cre transgenic mice ruled out the dorsal aorta as the source of the PAA endothelium (Li et al., 2012). Understanding the origin of endothelial progenitors giving rise to the PAAs is imperative for elucidating the mechanisms regulating PAA formation and alterations that lead to congenital heart disease.

Broadly, the anterior mesoderm, which includes the PAA endothelium arises from *Mesp1*-expressing progenitors during early gastrulation (Liang et al., 2014; Papangeli and Scambler, 2013). It is also known that a small proportion of the PAA endothelium expresses Nkx2.5 or derives from Nkx2.5-expressing progenitors (Paffett-Lugassy et al., 2013). However, a precise embryonic tissue that gives rise to the PAA endothelium in mice is unknown. It is also not known how endothelial progenitors are recruited into the pharyngeal arches and the mechanisms regulating the formation of PAA lumens.

In the studies described below, we determined that the PAA endothelium in the pharyngeal arches 3 – 6 arises from a subset of the splanchnic mesoderm within the *Mesp1* lineage. This subset is defined by the expression of the *Isl1* transcription factor and the Mef2C-AHF-Cre transgene and is known as the second heart field (SHF) (Evans et al., 2010; Verzi et al., 2005; Vincent and Buckingham, 2010). Using carefully-staged mouse embryos, we

demonstrate that cells within the SHF express *VEGFR2*, delaminate from the SHF, migrate into the pharyngeal mesenchyme, and form a plexus of small blood vessels, which then remodels into the PAA in each arch.

Mutations in *Tbx1*, *Gbx2*, *PlexinD1* and *Fgf8* interfere with PAA formation (Calmont et al., 2009; Gitler et al., 2004; Jerome and Papaioannou, 2001; Lindsay et al., 2001; Macatee et al., 2003; Merscher et al., 2001); However, which particular stages of PAA formation are regulated by these genes is unknown. Identification of PAA endothelial progenitors and cellular mechanisms regulating PAA formation are important steps toward understanding the etiology of congenital heart disease.

2.0 MATERIALS AND METHODS

2.1 Mouse strains

Cdh5(PAC)-CreERT2 transgenic mice were a gift from Dr. Ralph Adams (Wang et al., 2010). $Rosa^{mTmG}$ mice, Gt(ROSA)26Sortm4(ACTB-tdTomato–EGFP) generated by (Muzumdar et al., 2007) were purchased from Jackson Labs (stock number 007676). Tg(Mef2c-cre)2Blk/Mmnc strain, also known as the Mef2C-AHF-Cre transgenic mice (Verzi et al., 2005) were obtained from the Mutant Mouse Resource and Research Center (stock number 030262-UNC). The $Isl1^{Cre}$ strain was a gift from Sylvia Evans (Cai et al., 2003). All experimental procedures were approved by the Institutional Animal Care and Use Committee of Thomas Jefferson University and conducted in accordance with federal guidelines for humane care of animals.

2.2 Tracing endothelial lineage in pharyngeal arches

Tamoxifen solution (20 mg/ml) was prepared by dissolving Tamoxifen (Sigma, #T5648) in corn oil. The solution was heated at 40°C and rocked at 1000 rpm using Eppendorf Thermomixer® for 3 hours; insoluble particles were removed by centrifugation. To label endothelial cells with GFP prior to the formation of the PAAs 3 – 6, we crossed $ROSA^{mTmG}$ females with Cdh5(PAC)-CreERT2 transgenic males, and injected 4 mg of tamoxifen per 25g of body weight, into pregnant females in the morning (10–11am) of day E7.5. Embryos were dissected in the morning of day E9.5, and were subjected to whole mount staining with the antibodies against GFP (1:500, Aves labs, #GFP-1020) and VEGFR2 (1:200, R&D, #AF644). Nuclei were stained with DRAQ5. Stained embryos were then imaged using Olympus FV500 confocal microscope. Three-dimensional (3D) reconstructions and surface renderings were performed using Imaris (Bitplane, USA).

2.3 Whole-mount immunofluorescence staining and confocal image acquisition

Embryos at E9.5 or E10.5 were dissected and fixed at 4°C in 4% paraformadehyde overnight for ~ 15 hours with gentle rocking. Embryos were then rinsed and washed with PBS every 30 min for 1 to 2 hours. The number of somites (s) was counted in each embryo analyzed. Prior to staining, the head, forelimb buds and trunk posterior to the forelimb buds in E10.5 embryos were trimmed off. E9.5 embryos and younger were used without trimming. During all incubations, embryos were kept in 2 ml eppendorf tubes (Fisherbrand, #02-681-258), with 1 embryo per tube. Embryos were first incubated in 500 μl of blocking buffer (PBS

with 0.1% Triton X100 and 10% Donkey serum) overnight at 4°C with gentle rocking, then with 450 μl of blocking buffer containing 1° antibodies for 72 hours at 4°C, with gentle rocking. The following 1° antibodies were used: anti-PECAM1 (BD Pharmingen, #553370, 1:200), anti-VEGFR2 (R&D, AF644, 1:200), anti-ERG (Abcam, ab110639, 1:100), and anti-GFP (Aves lab, #GFP1020, 1:500). After the incubation with 1° antibodies, embryos were rinsed and washed every hour with PBST (PBS with 0.1% Triton X100) for at least 5 hours. Embryos were then incubated with 450 μl of 2° antibodies diluted 1:300 in blocking buffer for 48 hours at 4°C. Alexa-labeled 2° antibodies were purchased from Invitrogen. FITC conjugated anti-chicken IgY antibodies were from Jackson Immunoresearch, #703-546-155. After staining with 2° antibodies, embryos were washed as above, and incubated with DRAQ5 (1:500 dilution in PBST, Cell signaling technology, #4048) for 48 hours to stain nuclei. This extra incubation step was necessary because the presence of serum in the blocking buffer interferes with DRAQ5 staining. Prior to imaging, embryos were dehydrated in 50% methanol in PBS for 5 minutes, followed by 100% methanol two times for 5 minutes each, and cleared in BABB generated by mixing benzyl alcohol (Sigma, #B1042) and benzyl benzoate (Sigma, #B6630) at 1:2 (v/v). This procedure eliminates the native GFP and tdTomato fluorescence from $ROSA^{mTmG}$ mice, allowing the use of any combination of the fluorophores described above. Images of entire pharyngeal arches were acquired with Olympus FV500 confocal microscope, collecting optical sections every 0.62 μm through the entire thickness of the embryo.

2.4 3D quantitative analyses of confocal images

Overall, we analyzed 6 pharyngeal arches from embryos having 30 – 31 somites (s), 16 pharyngeal arches from embryos having 33 – 34 s, and 10 pharyngeal arches from embryos with 36 – 39 s. 3D image reconstruction and analyses of cell numbers and distributions were performed using Imaris, and the methodology is illustrated in Sup. Figs. 1 – 2. To label and quantify the number of endothelial cells in the PAA and plexus of the 4^{th} arch, we used the surface function in Imaris to create a segment encompassing the 4^{th} pharyngeal arch, excluding all other regions (Sup. Fig. 1A – C). We then generated a new channel encompassing all of the endothelial cells within this segment (Sup. Fig. 1D, region in red). To separate the PAA endothelium from the plexus, we segmented the pharyngeal arch artery endothelium as shown in Sup. Fig. 1F – G and generated a new surface containing $Pecam1^{+}$ cells within the PAA (Sup. Fig. 1H). We then generated a new channel containing endothelial cells in the PAA (Sup. Fig. 1I, PAA). The channel with plexus endothelial cells was generated by excluding endothelial cells in the PAA (Sup. Fig. 1J). To quantify the number of endothelial cells, ERG^{+} nuclei within these channels were counted using the Spots function in Imaris, as illustrated in Sup. Fig. 2. This number was confirmed by manual counting in several samples.

The number of SHF-derived endothelial cells in each PAA was quantified in 4 E10.5 embryos, ranging from 33s to 35s, 2 of these embryos were from the $Isl1^{Cre}$; $Rosa^{mTmG}$ strain and the other 2 embryos were from the Mef2C-AHF-Cre; $Rosa^{mTmG}$ strain. All embryos were stained with antibodies to GFP, VEGFR2 and ERG, and pharyngeal arches were imaged using confocal microscopy, collecting optical sections through the entire thickness of the embryo, sampling every 0.62 μm. The number of GFP^{+} and GFP^{-}

endothelial cells in each pharyngeal arch was determined in optical sections spaced 15 – 20 microns, using the Imaris software. A total of 707 endothelial cells were examined in the 3rd PAAs, 589 endothelial cells were analyzed in the 4th PAAs, and 370 endothelial cells were analyzed in the 6th PAAs. The results of these analyses were plotted in Fig. 2B‴, and statistical significance was determined using 2-way ANOVA and the GraphPad Prism 6 software.

2.5 Staining of tissue sections

For frozen sections, fixed embryos were rinsed in PBS and incubated in 30% sucrose solution prepared in PBS until embryos sunk to the bottom of the tube. This was followed by incubation in 50/50 mix of 30% sucrose solution and optimum cutting temperature (OCT) compound (Tissue-Tek) at 4°C overnight. Embryos were then embedded in OCT and frozen using an isopentane/dry ice bath. The following primary antibodies were diluted in blocking buffer (10% donkey serum, PBS, 0.05% Tween-20) and used to stain frozen sections overnight at 4°C: anti-VEGFR2 (1:200, R&D, #AF644), anti-ERG (1:100, Abcam, #ab110639), anti-GFP (1:500, Aves labs, #GFP-1020), and anti-Cre (1:500, Millipore, #MAB3120). Slides were washed in PBS containing 0.05% Tween 20 (PBS-Tween) with three changes of washing buffer, 10 min each, and then incubated with Alexa-conjugated 2° antibodies, diluted 1:300 in blocking buffer for 2 hours at room temperature. After washing in PBS-Tween, sections were mounted using a 1:1 mixture of methanol and glycerol (v/v) to extinguish the native GFP and tdTomato fluorescence. Slides were imaged using Olympus FV500 confocal microscope. Each experiment was repeated at least three times, using 3 independent embryos.

2.6 Cell proliferation

5 mg/ml BrdU solution was prepared by dissolving BrdU (Fisher Scientific, # BP2508250) in PBS. BrdU (30mg per kg of body weight) was injected intraperitoneally into pregnant females 30 minutes before they were sacrificed. 66 sections from 10 pharyngeal arches (5 right and 5 left) were analyzed. Paraffin sections were stained with anti-ERG and anti-BrdU antibodies (Abcam, #ab6326, 1:100) after antigen retrieval with 10 mM citric acid buffer, pH 6.0. Alexa-labeled secondary antibodies were used to detect the bound 1° antibodies, and nuclei were visualized using DRAQ5.

2.7 Cell survival

Anti-cleaved caspase-3 antibody (1:100, Cell Signaling Technology, #9661) was used to detect apoptosis in whole embryos (5 embryos were analyzed using whole-mount staining followed by confocal scanning, and an additional 3 embryos were sectioned to perform the TUNEL assay). Whole mount immunofluorescence staining and imaging were performed as described above. In Situ Cell Death Detection Kit, Fluorescein TUNEL was purchased from Roche (#11684795910). TUNEL labeling was performed using cryosections according to the manufacturer's instructions.

3.0 RESULTS AND DISCUSSION

3.1 Endothelium of the PAAs 3 – 6 is not derived from the dorsal aorta, endocardium, or the aortic sac

By 18 somites (s) of mouse development, pharyngeal endothelial cells are present as a uniform plexus within the region corresponding with the future arches 3 – 6 (Li et al., 2012). To determine whether the endothelium in these pharyngeal arches arose from the dorsal aorta, the aortic sac, or the endocardium, we performed transient lineage labeling studies with the aim of labeling the endocardium and endothelium prior to the formation of the PAAs 3 – 6. If pharyngeal endothelial cells were derived from the dorsal aorta, aortic sac, endocardium, or from an earlier progenitor in common with these vascular beds, they would express GFP due to the presence of the *ROSA*^{mTmG} reporter. For these experiments, *ROSA*^{mTmG} females were crossed with Cdh5(PAC)-CreERT2 transgenic males, in which the expression of tamoxifen-inducible Cre recombinase in the endothelium is driven by the *Cdh5* regulatory elements (Wang et al., 2010). Pregnant females were injected with tamoxifen at E7.5. The half-life of tamoxifen in serum is ~12 hours (Robinson et al., 1991), and Cre-mediated expression of a reporter becomes detectable in 95% of cells within the first 24 hours after injection (Hayashi and McMahon, 2002). Thus, the injection of tamoxifen at E7.5 allows labeling of blood vessels formed by E8.5. These vessels include the endothelium of the dorsal aortae, the aortic sac, the ventral aortae (discussed in more details below), and the endocardium; but not the pharyngeal arteries 3 – 6, which are not present at that time.

We dissected labeled embryos at E9.0, 48 hours after the injection of tamoxifen, and performed whole mount confocal immunofluorescence microscopy followed by 3D image reconstruction. In these and all other imaging experiments, we inactivated the native GFP and tdTomato fluorescence by clearing embryos with methanol and BABB (see Methods). Endothelial cells were visualized using anti-VEGFR2 antibody, GFP was detected using anti-GFP antibody, and nuclei using DRAQ5. Confocal imaging of whole embryos shows that the injection of tamoxifen at E7.5 leads to the expression of GFP in the endocardium of the heart (h in Fig. 1A – C, 1I), in the dorsal aorta (da in Fig. 1D– H2, J – J2), and in the aortic sac (Fig. 2I and Sup. Movie 1). The endothelium of the ventral aortae is also GFP^{+} (Fig. 1I – H2, see further discussion of the ventral aortae in **Section 3.3**). Interestingly, the majority of endothelial cells in the pharyngeal region corresponding with the future arches 3, 4 and 6 are GFP^{-} (see the region circumscribed by the dashed line in Fig. 1D – F and surface-rendered in Fig. 1G). In contrast, the endothelium of the 1st and 2nd PAAs and that of intersomitic arteries are GFP^{+} (Fig. 1A – C, Sup. Movie 1). Intersomitic arteries arise from the dorsal aorta by angiogenesis (Coultas et al., 2005). Thus, the labeling of the 1st and 2nd PAAs and the intersomitic arteries with GFP serves as the internal positive control for vessels that either arose from the dorsal aorta or have progenitors in common with the dorsal aorta. Alternatively, as is the case with the 1st and 2nd PAAs, the GFP labeling of these PAAs occurred because these vessels/endothelial cells were present contemporaneously with the injected tamoxifen.

Even though tamoxifen mediated extensive labeling of the dorsal and ventral aortae, the endocardium, the aortic sac endothelium, and the endothelium in the 1st and 2nd pharyngeal arches in Cdh5(PAC)-CreERT2 transgenic embryos, endothelial cells in the pharyngeal arches 3 – 6 lacked GFP labeling (Fig. 1A – F and 1H1 – H2). The only GFP^+ cell seen in this region (Fig. 1D – G) is derived from the common cardinal vein (Fig. 1F, Sup. Fig. 3, and Sup. Movie 2). Nearly all, 95 of 102, endothelial cells in the dorsal aorta were GFP^+ (transverse and sagittal optical slices in Fig. 1H1 – J2). Similarly, nearly all endothelial cells in the heart, the aortic sac and the ventral aortae were also GFP^+ (Fig. 1I, 1H1 – H2 and Sup. Movie 1, showing all sagittal optical sections through the embryo). The absence of GFP^+ cells in the endothelium within the pharyngeal arch region 3 – 6 (with the exception of one GFP^+ cell) suggests that the pharyngeal endothelium in arches 3 – 6 is derived from a source other than the dorsal aortae, the aortic sac, the ventral aortae or the endocardium.

3.2 PAA endothelial cells arise from the second heart field

The high dose of tamoxifen used in the experiments described above was necessary to achieve efficient cell labeling; however, its toxicity precluded examination of embryos at later time points. To complement these experiments and to identify the major source of endothelial cells in the PAAs 3 – 6, we used lineage tracing. Our earlier studies and the work of others showed that the majority of PAA endothelial cells in mice are derived from *Mesp1*$^+$ precursors (Liang et al., 2014; Papangeli and Scambler, 2013). We also found that the majority of PAA endothelial cells express *Isl1* in embryos older than 36s (Chen et al., 2015), suggesting that PAA endothelial cells could have been derived from the second heart field (SHF) mesoderm. However, the expression of the Isl1 protein in the PAA endothelium does not indicate lineage. To determine whether precursors of the PAA endothelium originate in the SHF, we analyzed embryos from the Mef2C-AHF-Cre transgenic mice at different stages of development (Verzi et al., 2005). The Mef2C-AHF enhancer drives the expression of Cre exclusively in the SHF (Dodou et al., 2004; Verzi et al., 2005). Examination of GFP^+ cells within the SHF in Mef2C-AHF-Cre; $Rosa^{mTmG}$ embryos at 24s demonstrated that many SHF cells express VEGFR2 (Fig. 2A – A″), extend cellular processes toward the gut endoderm, and appear to be emigrating from the SHF and joining with the pharyngeal endothelial plexus (arrowheads in 2A″). Patent PAAs 3 – 6 are formed by E10.5 (≥33s), and at this time, the majority of endothelial cells in the PAAs 3 – 6 are GFP^+ (Fig. 2B – B‴). To determine whether GFP^+ cells in the PAAs 3 – 6 were related to the SHF by lineage, we stained sections with antibodies against the Cre recombinase. Although Cre is expressed in the SHF (arrowheads and red signal in Fig. 2B, B″), it is not expressed in the majority of the GFP^+ PAA endothelium (Fig. 2B′ – B″), indicating that the expression of GFP in the PAA endothelium represents a true fate map. In contrast, endothelial cells in the first and second pharyngeal arches were mostly GFP^- in Mef2C-AHF-Cre; $Rosa^{mTmG}$ embryos, while the mesodermal core of these arches was GFP^+ (see Figs. 2C – C″, 2C1 – 2C1″ for E10.5 embryos and Fig. 4A – B″ for E9.5 embryos). This is consistent with the labeling experiments in Fig. 1, and supports the notion that the endothelium in the pharyngeal arches 1 and 2 arose earlier and is of different origin than the endothelium in the PAAs 3 – 6.

Quantitatively, SHF contributes to 90+/−10% of endothelial cells in the 3rd PAAs, 95+/−5% of endothelial cells in the 4th PAAs, and 91+/−11% of endothelial cells in the 6th PAAs at E10.5 (Fig. 2B‴). The contribution of SHF-derived cells to the left PAAs 3 – 6 was slightly higher than to the right PAAs (Fig. 2B‴, p=0.03, 2-way ANOVA).

Symmetrical PAAs become remodeled into the AAAs by E13.5. To determine whether the AAAs retain the SHF-derived endothelium, we analyzed transverse and coronal sections through Mef2C-AHF-Cre;ROSA^{mTmG} embryos isolated at E15.5 and E16.6. We found that indeed, the endothelium of the carotid arteries, which are derived from the left and right 3rd PAAs is GFP^{+} (Fig. 2D, rCA, lCA). Similarly, endothelial cells of the ductus arteriosus, which is derived from the left 6th PAA (Fig. 2E) and endothelial cells of the aortic arch, which is derived from the left 4th PAA are GFP^{+} (Fig. 2F – F″). The short proximal portion of the right subclavian artery is derived from the right 4th PAA, and have not been analyzed here. The right 6th PAA completely degenerates during the remodeling of the PAAs into the AAAs. Together, these experiments demonstrate that the AAA endothelium is mainly composed of SHF-derived cells.

3.3 SHF progenitors giving rise to the aortic sac and the PAAs are temporally and spatially distinct

The aorta and the pulmonary trunk arise from the OFT and the aortic sac, which connects the OFT with the PAAs (Waldo et al., 2005a; Waldo et al., 1996). Fate mapping studies show that the endothelium of the OFT and the aortic sac is derived from the SHF (Cai et al., 2003; Sun et al., 2007; Verzi et al., 2005). The endothelium of the aorta and pulmonary trunk is also derived from the SHF (Fig. 2F – F″). Despite the fact that the endothelium of the OFT and the PAAs 3 – 6 is SHF-derived, morphological and fate-mapping data discussed below argue that the aortic sac does not give rise to the PAA endothelium. To see this, we first need to consider endothelial components in the developing pharyngeal region, which were first described over a century ago by John Lewis Bremer (Bremer, 1912).

Bremer noted the presence of two vessels on either side of the midline, located dorsal to the OFT, and running along the embryo's anterior-posterior axis (Bremer, 1912). These vessels, which Bremer referred to as the ventral aortae, connect the arterial pole of the heart with the nascent 1st and 2nd PAAs anteriorly and with the developing PAAs 3 – 6th posteriorly (Bremer, 1912). Using Imaris and confocal immunofluorescence microscopy of Mef2C-AHF-Cre;ROSA^{mTmG} embryos labeled with antibodies to VEGFR2 and GFP, we generated a 3D reconstruction of the ventral aortae extending posteriorly from the heart of the 25-somite mouse embryo (E9.5) (Fig. 3A – A′). The region encompassing the ventral aortae (marked by arrows in Fig. 3A – A′) becomes incorporated into the OFT, as shown by dye injection experiments in chick (Waldo et al., 2005a; Waldo et al., 2005b; Waldo et al., 2001). Sagittal sections through the ventral aorta of Mef2C-AHF-Cre;ROSA^{mTmG} embryos show that the endothelium of the ventral aorta is connected with the OFT anteriorly and expresses GFP (Fig. 3A″). The ventral aortae extending posteriorly from the OFT are lumenized prior to the formation of patent 3rd, 4th and 6th PAAs (Fig. 1H1, H2 and transverse sections in Fig. 3). By 33s, the ventral aorta on each side of the midline is connected with the PAAs (Fig.

3B1 – B3) and gives rise to the aortic sac connecting all the posterior PAAs with the OFT by 35s (Fig. 3C – C′).

Several lines of evidence indicate that PAAs do not arise from the ventral aortae or the aortic sac: ***1)*** The aortic sac and ventral aortae are extensively labeled with GFP in Cdh5(PAC)-CreERT2;ROSA^{mTmG} transgenic embryos upon the injection of tamoxifen at E7.5 (short straight arrows in Fig. 1I, H1 – H2), while endothelial cells in the future pharyngeal arches 3 – 6 are not labeled (Fig. 1A– G, H1 – H2); This indicates that the endothelium of the pharyngeal arch arteries arises later than that of the aortic sac/ventral aortae; ***2)*** The ventral aortae are connected with the OFT and are lumenized before they form connections with the endothelial plexus of the future PAAs 3 – 6 (Fig. 1I, H1 – H2 and transverse level ii in Fig. 3). Finally, the paired ventral aortae form medially, while the PAA endothelium forms laterally relative to the midline (Fig. 1H1 – 2, Fig. 3A′, A″ and transverse sections in Fig. 3). In summary, these data show that SHF-derived progenitors giving rise to the endothelium of the ventral aortae and the aortic sac are spatially and temporally distinct from the SHF progenitors that give rise to the PAA endothelium in the pharyngeal arches 3 – 6. Together with the studies demonstrating early separation of the myocardial and endothelial lineages in the heart, our work suggests that the SHF consists of several populations of progenitor cells, that are temporally and/or spatially distinct (Devine et al., 2014; Jain et al., 2015; Milgrom-Hoffman et al., 2011). Some of these progenitors give rise to the myocardium, while others give rise to the endothelial cells of the OFT, ventral aortae, aortic sac and the PAAs.

3.4 Connections of the PAAs with the dorsal aorta

At E9.0, when the connections between the pharyngeal plexus endothelium and the dorsal aortae are minimal, we find that there is only a small number of GFP^{+} cells in the dorsal aorta of Mef2C-AHF-Cre; Rosa^{mTmG} embryos (Fig. 4A, A″, arrowheads). These GFP^{+} cells are located at sites, where the dorsal aorta fuses with the pharyngeal endothelial plexus (Fig. 4B – B″, arrow). At E10.5, when the connections between the PAAs with the dorsal aortae are well-formed, we observe extensive GFP labeling of the the dorsal aortae adjacent to the PAAs (Fig. 4C – C″, arrows) and increased numbers of GFP^{-} endothelial cells in the portions of the PAAs proximal to the junctions of the PAAs with the dorsal aortae (Fig. 4D – D″, arrowhead). We hypothesize that GFP^{-} cells at the PAA – dorsal aorta junctions migrate from the dorsal aorta to join with the PAA endothelium, and vice versa, that GFP^{+} cells at the ventral surface of the dorsal aorta arise from the PAA endothelium. This hypothesis is consistent with the observation that endothelial cells are highly motile, and that they can move within and between blood vessels (Culver and Dickinson, 2010; Lucitti et al., 2007; Sato et al., 2010).

3.5 PAAs form by the coalescence of the pharyngeal arch endothelium

Our studies demonstrated that pharyngeal plexus endothelium is derived from the SHF, as is the PAA endothelium (Figs. 2, 4). This indicates that the PAAs arise by remodeling the pharyngeal endothelial plexus, as was proposed by earlier studies (Bremer, 1912; Congdon, 1922; DeRuiter et al., 1993a; DeRuiter et al., 1993b; DeRuiter et al., 1992; Li et al., 2012; Waldo et al., 1996). To further understand the cellular mechanisms regulating PAA formation, we focused on the 4th pair of PAAs, and used whole-mount confocal

immunofluorescence microscopy to image these PAAs in carefully staged embryos (for the details about surface rendering and quantification methods see Sup. Figs. 1 – 2). At 30s – 31s, in the morning of E10.5, the endothelium in the pharyngeal region corresponding with the arches 4 and 6 is assembled into a uniform, non-hierarchical plexus of blood vessels (Fig. 5A – B). This plexus starts to rearrange between 30s and 34s, such that a nascent, thin PAA is seen by the 33rd somite stage in the 4th pharyngeal arch (Fig. 5C – D). The 4th PAA grows with time (Fig. 5E – F) and is visibly in larger diameter than the surrounding endothelial plexus (Fig. 5D – F). By the evening of E10.5, when embryos reach 36s – 39s, a prominent, large PAA is seen in the 4th pharyngeal arch (Fig. 5G – H).

We found that the number of endothelial cells in the 4th pharyngeal arch increases more than 2-fold between 30s and 39s (Fig. 5I). As the 4th PAA grows in diameter and length, the proportion of endothelial cells in the PAA increases, while the proportion of endothelial cells in the plexus decreases (Fig. 5J): at 30s – 31s, all endothelial cells in the 4th arch are in the plexus of interconnected small vessels; at 33s – 34s, endothelial cells are distributed equally between the PAA and the plexus; and at 36s–39s, 57% of endothelial cells are in the PAA and 43% in the plexus, $p=2\times10^{-4}$. Apoptosis is minimal in the pharyngeal endothelium of the 4th arch at this time (Fig. 6). Despite the decrease in the fraction of plexus endothelium in the pharyngeal arch (Fig. 5J, pink line), the proliferation index of plexus endothelial cells is ~2-fold higher than that of PAA endothelial cells, $p<10^{-4}$ (compare pink and green bars in Fig. 5K). These analyses suggest that the 4th pair of PAAs grows both by proliferation and by the acquisition of endothelial cells from the plexus. Indeed, sagittal sections show that the plexus endothelium is connected with the growing PAA (arrowheads in Fig. 5D, F, H).

Understanding genes and mechanisms regulating the formation of the 4th PAA is of particular clinical relevance, since aberrant formation of the left 4th PAA gives rise to the interruption of the aortic arch type B, a lethal congenital defect. While a number of genes are already known to regulate the formation of the 4th pair of PAAs, how they do so is not clear. Identification of the progenitors of PAA endothelium in the 4th pharyngeal arches, their embryonic origin, and cellular dynamics regulating PAA formation are significant advances in the understanding of developmental processes regulating PAA formation. Our works shows that PAA formation could be regulated at a number of distinct steps, which include differentiation, proliferation, and survival of VEGFR2^{+} PAA progenitors in the SHF; exit and migration of these progenitors from the SHF into the pharyngeal mesenchyme; formation of endothelial plexus, and the coalescence of the pharyngeal plexus endothelium into the large PAA in each pharyngeal arch. Thus, our studies establish a platform for elucidating physiological mechanisms regulating PAA formation and for analyzing mutants that interfere with this process.

Supplementary Material

Refer to Web version on PubMed Central for supplementary material.

Acknowledgments

We are grateful to Ralph Adams for Cdh5(PAC)-CreERT2 transgenic mice and to Nancy Speck for supplying these mice to our lab; We thank Brian Black for the Mef2C-AHF-Cre transgenic strain and Sylvia Evans for the *Isl1*^{Cre}

strain. We grateful to Mary Hutson for help with identifying the ventral aortae and for pointing to the earlier literature on the subject, Karl Degenhardt for help with labeling the great vessels in late gestation embryos, and Nathan Astrof for careful reading of the manuscript and discussion. We thank Jennifer Wilson from the TJU Writing Center for editorial assistance. This work was supported by the funding from the National Heart, Lung and Blood Institute of the NIH, grant HL103920 to S.A. AJR is supported by the National Institute of Arthritis and Musculoskeletal and Skin Diseases of the NIH under Award Number T32052283-11.

References

Bremer JL. The development of the aorta and aortic arches in rabbits. American journal of anatomy. 1912; 13:111–128.

Cai CL, Liang X, Shi Y, Chu PH, Pfaff SL, Chen J, Evans S. Isl1 identifies a cardiac progenitor population that proliferates prior to differentiation and contributes a majority of cells to the heart. Dev Cell. 2003; 5:877–889. [PubMed: 14667410]

Calmont A, Ivins S, Van Bueren KL, Papangeli I, Kyriakopoulou V, Andrews WD, Martin JF, Moon AM, Illingworth EA, Basson MA, Scambler PJ. Tbx1 controls cardiac neural crest cell migration during arch artery development by regulating Gbx2 expression in the pharyngeal ectoderm. Development. 2009; 136:3173–3183. [PubMed: 19700621]

Chen D, Wang X, Liang D, Gordon J, Mittal A, Manley N, Degenhardt K, Astrof S. Fibronectin signals through integrin alpha5beta1 to regulate cardiovascular development in a cell type-specific manner. Dev Biol. 2015; 407:195–210. [PubMed: 26434918]

Congdon ED. Transformation of the aortic arch system during the development of the human embryo. Contributions to Embryology. 1922; 14:47–110.

Coultas L, Chawengsaksophak K, Rossant J. Endothelial cells and VEGF in vascular development. Nature. 2005; 438:937–945. [PubMed: 16355211]

Culver JC, Dickinson ME. The effects of hemodynamic force on embryonic development. Microcirculation. 2010; 17:164–178. [PubMed: 20374481]

DeRuiter MC, Gittenberger-de Groot AC, Poelmann RE, VanIperen L, Mentink MM. Development of the pharyngeal arch system related to the pulmonary and bronchial vessels in the avian embryo. With a concept on systemic-pulmonary collateral artery formation. Circulation. 1993a; 87:1306–1319. [PubMed: 8462154]

DeRuiter MC, Poelmann RE, Mentink MM, Vaniperen L, Gittenberger-De Groot AC. Early formation of the vascular system in quail embryos. Anta Reek. 1993b; 235:261–274.

DeRuiter MC, Poelmann RE, Banderoles-de Varies I, Mentink MM, Gittenberger-de Groot AC. The development of the myocardium and endocardium in mouse embryos. Fusion of two heart tubes? Anta Embryo (Burl). 1992; 185:461–473.

Devine WP, Wither JD, George M, Toshiba-Takeuchi K, Bureau BG. 2014Early patterning and specification of cardiac progenitors in gastrulating mesoderm. elite. :3.

Dodou E, Verzi MP, Anderson JP, Up SM, Black BL. Mef2c is a direct transcriptional target of ISL1 and GATA factors in the anterior heart field during mouse embryonic development. Development. 2004; 131:3931–3942. [PubMed: 15253934]

Evans SM, Felon D, Conlon FL, Kirby ML. Myocardial lineage development. Circ Rees. 2010; 107:1428–1444.

Gitler AD, Lu MM, Epstein JA. PlexinD1 and semaphoring signaling are required in endothelial cells for cardiovascular development. Dev Cell. 2004; 7:107–116. [PubMed: 15239958]

Hayashi S, McMahon AP. Efficient recombination in diverse tissues by a tamoxifen-inducible form of Cre: a tool for temporally regulated gene activation/inactivation in the mouse. Dev Biol. 2002; 244:305–318. [PubMed: 11944939]

Hiruma T, Nakajima Y, Nakamura H. Development of pharyngeal arch arteries in early mouse embryo. J Anta. 2002; 201:15–29.

Hutson MR, Kirby ML. Model systems for the study of heart development and disease. Cardiac neural crest and conotruncal malformations. Semin Cell Dev Biol. 2007; 18:101–110. [PubMed: 17224285]

Jain R, Li D, Gupta M, Manderfield LJ, Ifkovits JL, Wang Q, Liu F, Liu Y, Poleshko A, Padmanabhan A, Raum JC, Li L, Morrisey EE, Lu MM, Won KJ, Epstein JA. HEART DEVELOPMENT.

Integration of Bmp and Wnt signaling by Hopx specifies commitment of cardiomyoblasts. Science. 2015; 348:aaa6071. [PubMed: 26113728]

Jerome LA, Papaioannou VE. DiGeorge syndrome phenotype in mice mutant for the T-box gene, Tbx1. Nat Genet. 2001; 27:286–291. [PubMed: 11242110]

Li P, Pashmforoush M, Sucov HM. Mesodermal retinoic acid signaling regulates endothelial cell coalescence in caudal pharyngeal arch artery vasculogenesis. Dev Biol. 2012; 361:116–124. [PubMed: 22040871]

Liang D, Wang X, Mittal A, Dhiman S, Hou SY, Degenhardt K, Astrof S. Mesodermal expression of integrin alpha5beta1 regulates neural crest development and cardiovascular morphogenesis. Dev Biol. 2014; 395:232–244. [PubMed: 25242040]

Lindsay EA, Vitelli F, Su H, Morishima M, Huynh T, Pramparo T, Jurecic V, Ogunrinu G, Sutherland HF, Scambler PJ, Bradley A, Baldini A. Tbx1 haploinsufficieny in the DiGeorge syndrome region causes aortic arch defects in mice. Nature. 2001; 410:97–101. [PubMed: 11242049]

Lucitti JL, Jones EA, Huang C, Chen J, Fraser SE, Dickinson ME. Vascular remodeling of the mouse yolk sac requires hemodynamic force. Development. 2007; 134:3317–3326. [PubMed: 17720695]

Macatee TL, Hammond BP, Arenkiel BR, Francis L, Frank DU, Moon AM. Ablation of specific expression domains reveals discrete functions of ectoderm- and endoderm-derived FGF8 during cardiovascular and pharyngeal development. Development. 2003; 130:6361–6374. [PubMed: 14623825]

Merscher S, Funke B, Epstein JA, Heyer J, Puech A, Lu MM, Xavier RJ, Demay MB, Russell RG, Factor S, Tokooya K, Jore BS, Lopez M, Pandita RK, Lia M, Carrion D, Up H, Schorle H, Kobler JB, Scambler P, Wynshaw-Boris A, Skoultchi AI, Morrow BE, Kucherlapati R. TBX1 is responsible for cardiovascular defects in velo-cardio-facial/DiGeorge syndrome. Cell. 2001; 104:619–629. [PubMed: 11239417]

Milgrom-Hoffman M, Harrelson Z, Ferrara N, Zelzer E, Evans SM, Tzahor E. The heart endocardium is derived from vascular endothelial progenitors. Development. 2011; 138:4777–4787. [PubMed: 21989917]

Muzumdar MD, Tasic B, Miyamichi K, Li L, Luo L. A global double-fluorescent Cre reporter mouse. Genesis. 2007; 45:593–605. [PubMed: 17868096]

Olson KR. Vascular anatomy of the fish gill. J Exp Zool. 2002; 293:214–231. [PubMed: 12115898]

Paffett-Lugassy N, Singh R, Nevis KR, Guner-Ataman B, O'Loughlin E, Jahangiri L, Harvey RP, Burns CG, Burns CE. Heart field origin of great vessel precursors relies on nkx2.5-mediated vasculogenesis. Nat Cell Biol. 2013; 15:1362–1369. [PubMed: 24161929]

Papangeli I, Scambler PJ. Tbx1 genetically interacts with the transforming growth factor-beta/bone morphogenetic protein inhibitor Smad7 during great vessel remodeling. Circ Rees. 2013; 112:90–102.

Robinson SP, Langan-Fahey SM, Johnson DA, Jordan VC. Metabolites, pharmacodynamics, and pharmacokinetics of tamoxifen in rats and mice compared to the breast cancer patient. Drug Metab Dispos. 1991; 19:36–43. [PubMed: 1673419]

Sato Y, Poynter G, Huss D, Filla MB, Czirok A, Rongish BJ, Little CD, Fraser SE, Lansford R. Dynamic analysis of vascular morphogenesis using transgenic quail embryos. PLoS One. 2010; 5:e12674. [PubMed: 20856866]

Sun Y, Liang X, Najafi N, Cass M, Lin L, Cai CL, Chen J, Evans SM. Islet 1 is expressed in distinct cardiovascular lineages, including pacemaker and coronary vascular cells. Dev Biol. 2007; 304:286–296. [PubMed: 17258700]

Verzi MP, McCulley DJ, De Val S, Dodou E, Black BL. The right ventricle, outflow tract, and ventricular septum comprise a restricted expression domain within the secondary/anterior heart field. Dev Biol. 2005; 287:134–145. [PubMed: 16188249]

Vincent SD, Buckingham ME. How to make a heart: the origin and regulation of cardiac progenitor cells. Current topics in developmental biology. 2010; 90:1–41. [PubMed: 20691846]

Waldo KL, Hutson MR, Stadt HA, Zdanowicz M, Zdanowicz J, Kirby ML. Cardiac neural crest is necessary for normal addition of the myocardium to the arterial pole from the secondary heart field. Dev Biol. 2005a; 281:66–77. [PubMed: 15848389]

Waldo KL, Hutson MR, Ward CC, Zdanowicz M, Stadt HA, Kumiski D, Abu-Issa R, Kirby ML. Secondary heart field contributes myocardium and smooth muscle to the arterial pole of the developing heart. Dev Biol. 2005b; 281:78–90. [PubMed: 15848390]

Waldo KL, Kumiski D, Kirby ML. Cardiac neural crest is essential for the persistence rather than the formation of an arch artery. Dev Dyn. 1996; 205:281–292. [PubMed: 8850564]

Waldo KL, Kumiski DH, Wallis KT, Stadt HA, Hutson MR, Platt DH, Kirby ML. Conotruncal myocardium arises from a secondary heart field. Development. 2001; 128:3179–3188. [PubMed: 11688566]

Wang Y, Nakayama M, Pitulescu ME, Schmidt TS, Bochenek ML, Sakakibara A, Adams S, Davy A, Deutsch U, Luthi U, Barberis A, Benjamin LE, Makinen T, Nobes CD, Adams RH. Ephrin-B2 controls VEGF-induced angiogenesis and lymphangiogenesis. Nature. 2010; 465:483–486. [PubMed: 20445537]

Highlights

- Endothelium in pharyngeal arches 3 – 6 arises from the second heart field
- Pharyngeal arch arteries (PAAs) form by vasculogenesis
- PAAs form by reorganization of pharyngeal arch endothelial cells

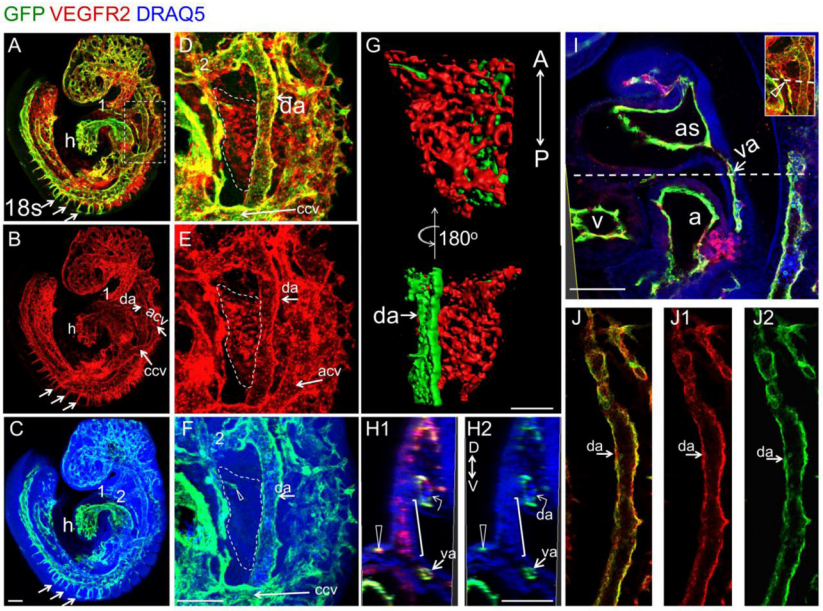

Figure 1. Endothelial cells of the PAAs 3 – 6 do not arise from the endocardium, the aortic sac, or dorsal and ventral aortae

Cdh5(PAC)-CreERT2; ROSA^{mTmG} embryos were treated with tamoxifen *in utero* and stained to detect GFP (green), VEGFR2 (red) and nuclei (DRAQ5). The native GFP and tdTomato fluorescence was extinguished by the treatment with methanol and BABB (see Methods). **A – C.** Low magnification views; 1, 2 – pharyngeal arch #1 and #2; three inclined arrows at the bottom of panels **A, B** and **C** point to intersomitic vessels. The region outlined by the dashed box in **A** is enlarged in **D – F. D – F.** Dashed perimeter circumscribes the pharyngeal region, where PAAs 3 – 6 will form. Pharyngeal plexus endothelial cells inside the dashed perimeter are VEGFR2^{+} but GFP^{-}. The lone GFP^{+} cell (arrowhead) seen inside the marked pharyngeal region is derived from the sprout branching from the common cardinal vein, ccv (**F** and Sup. Fig. 3 with Movie 2). **G.** Surface rendering of plexus endothelial cells (red – VEGFR2 channel, green – GFP channel) and the dorsal aorta (green – GFP channel). **H1 – H2.** Transverse optical section through the pharyngeal region at the level of the dashed line in **I** (see inset in **I** for the level relative to the embryo and the pharyngeal plexus). Plexus endothelial cells (brackets in **H1 – H2**) are VEGFR2^{+}GFP^{-}; da – dorsal aorta; straight arrows in **H1, H2** and **I** point to the cross section of the same vessel (the ventral aorta, va) at the level of the dashed line in **I**. Open arrowhead in **H1**, **H2** and in the inset of **I** point to the venous sprout. **H1** shows the overlay of VEGFR2 (red) and GFP (green); **H2** shows the GFP and DRAQ5 (blue) channels. **I.** Sagittal section through the heart shows that nearly all endothelial cells in the endocardium, the aortic sac, and the ventral aorta are labeled with GFP (see Movie 1 for all sagittal sections showing merged and single channels). Dashed line shows the level of the transverse section shown in **H. J – J2.** Sagittal optical sections showing that nearly all endothelial cells in the dorsal aorta express GFP. All scale bars are 100 μm, except in **G – H**, where they are 50 μm; acv – anterior cardinal vein; ccv – common cardinal vein; da – dorsal aorta; h – heart; as – aortic sac; a – atrium; v – ventricle; va – ventral aorta.

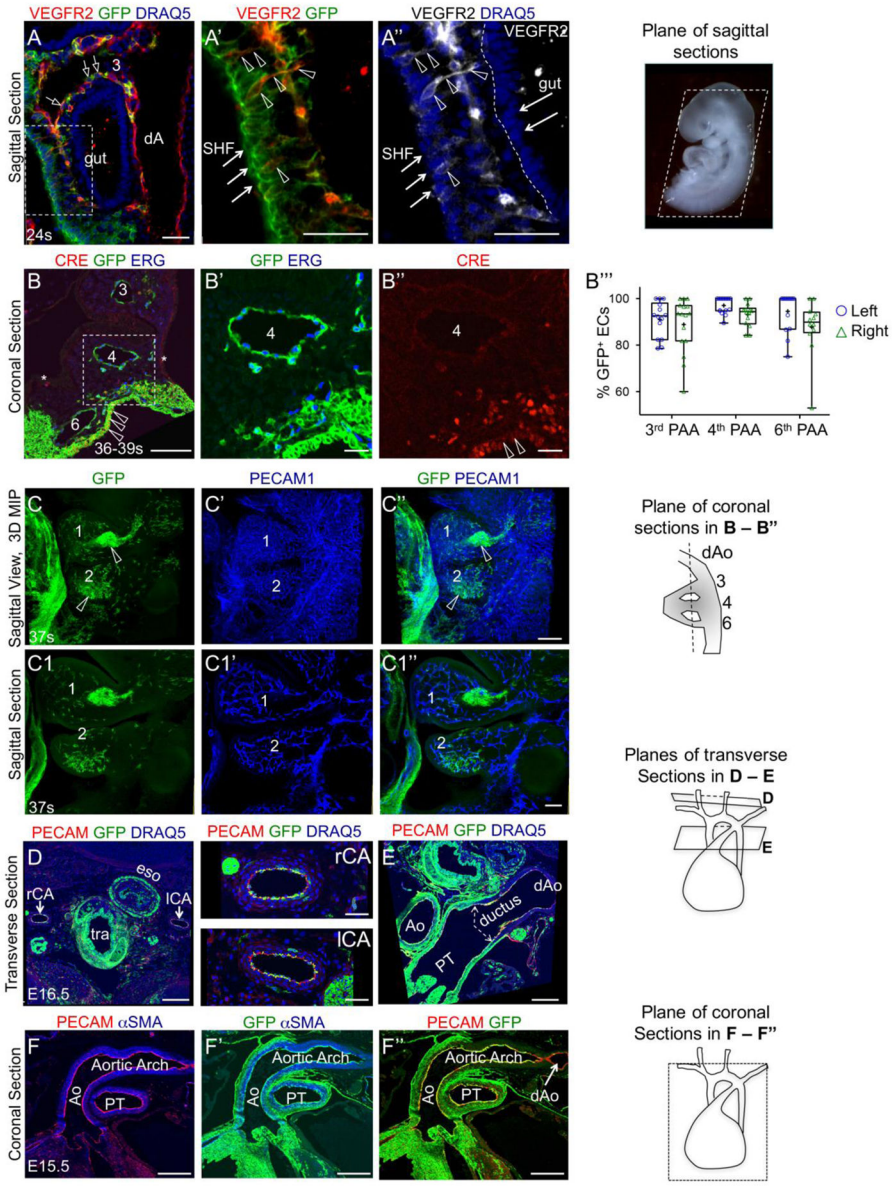

Figure 2. PAA endothelial cells are derived from the second heart field

Sections and 3D views in all panels are from Mef2C-AHF-Cre; ROSA^{mTmG} embryos dissected at E9.5, 24 somites (**A – A″**), at E10.5, 36–39 somites (**B – B″, C – C″, C1 – C″**), at E16.5 (**D – E**), or at E15.5 (**F – F″**). The native GFP and tdTomato fluorescence was extinguished by the treatment with methanol. PAAs are numbered. **A – A″.** Sagittal optical sections. The 3rd PAA is formed by 24s. The boxed region containing the SHF is expanded in **A′ – A″**. Open arrows in **A** mark GFP^{+}VEGFR2^{+} endothelial cells in the 3rd PAA. **A′ – A″**. Arrow in mark the SHF and arrowheads in mark GFP^{+}VEGFR2^{+} endothelial progenitors that appear emigrating from the SHF. The VEGFR2^{+} cell marked by three open arrowheads in **A′** and **A″** is seen extending a long process toward the endoderm. **B – B‴**. Nearly all endothelial cells in the PAAs 3 – 6 (ERG^{+}) are derived from Mef2C-AHF-Cre^{+} progenitors (GFP^{+}). The box in **B** is expanded in **B′ – B″**. Note the expression of Cre in the

lateral plate mesoderm (open arrowheads in **B, B″**) and the lack of Cre expression in the majority of endothelial cells of the 4th PAA, **B″**. Asterisks in **B** mark non-specific staining (red channel). **B‴**. Quantification of GFP^+ cells in sagittal optical sections from 2 Mef2C-AHF-Cre; $ROSA^{mTmG}$ and 2 $Isl1^{Cre}$; $ROSA^{mTmG}$ embryos, representing 4 pharyngeal arch arteries of each kind. Each data point corresponds with one optical sagittal section; all data points are plotted. Vertical lines span minimum to maximum, "+" marks the mean of each distribution, box includes the middle 50% of data. The difference in the % of GFP^+ endothelial cells between the left and right PAAs is significant, p=0.03, 2-way ANOVA. **C – C″**. 3D maximum intensity projections (MIP) of confocal stacks through the entire 1^{st} and 2^{nd} pharyngeal arches. Sagittal views are shown. The majority of endothelium in the 1^{st} and 2^{nd} arches at E10.5 is GFP^-, while the mesodermal cores (arrowheads) are GFP^+. **C1 – C1″**. Sagittal optical sections through the images shown in **C – C″. D**. The endothelium of the right and left carotid arteries is composed of GFP^+ cells, magnified in the adjacent panels. **E**. The endothelium of ductus arteriosus is GFP^+. The border of the pulmonary trunk and the ductus arteriosus is marked by the dashed double-headed arrow. **F – F″.** The endothelium of the aorta and pulmonary trunk is GFP^+. Ao – aorta; dA – dorsal aorta; dAo – descending aorta, lCA and rCA – left and right carotid arteries; eso – esophagus, MIP – maximum intensity projection, PT – pulmonary trunk, SHF – second heart field; tra – trachea; Scale bars are 30 μm in **A – A″**, 100 μm in **B**, 30 μm in **B′ – B″**, 200 μm in **C – C1″**, **D**, **E** and **F – F″**; Scale bars in panels marked **rCA** and **lCA** are 50 μm.

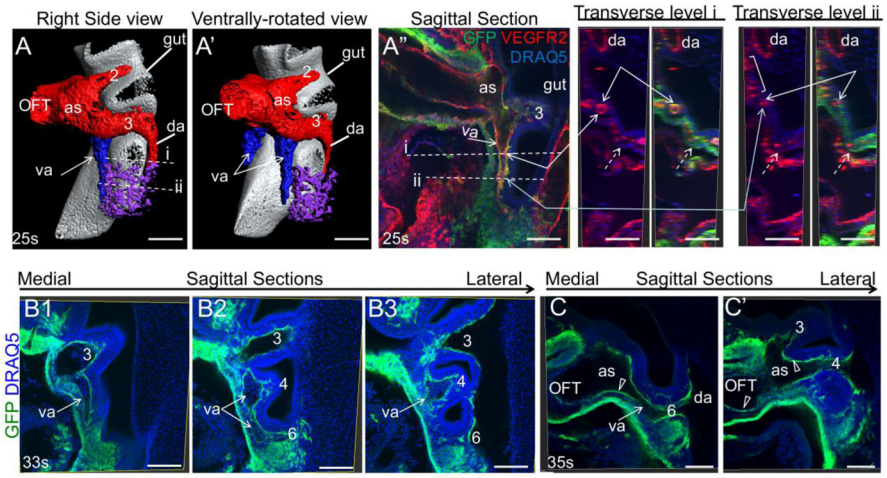

Figure 3. The relationship between the aortic sac, ventral aortae and PAAs

Panels show Mef2C-AHF-Cre; ROSA^{mTmG} embryos isolated at 25, 33 and 35 somites. **A – A′**. 25s. Surface rendering of blood vessels (VEGFR2^{+}) was done following whole mount confocal imaging; The endoderm (gut) was surfaced using the morphology of DRAQ5-stained nuclei. The OFT, aortic sac, dorsal aorta, 2nd and 3rd PAAs are surfaced in red; The ventral aortae are blue; Endothelial plexus of the 4th and 6th PAAs is purple. Dashed lines **i** and **ii** mark the planes of transverse sections shown on the right. **A″**. Sagittal section through the embryo in **A – A′**. The endothelium of the ventral aorta is GFP^{+}. Dotted lines show the planes of optical transverse sections (as in **A**). Transverse sections at the levels **i** and **ii** demonstrate that ventral aorta is lumenized prior to the formation of the 4th and 6th PAAs. Double-headed arrows point to the cross section of the same vessel, at the level indicated. Bracket in the transverse section **ii** marks pharyngeal endothelial plexus. Note that pharyngeal endothelial plexus at this level is not yet connected with the ventral aorta. **B1 – B3.** 33s. Connections between ventral aorta and the 3rd, 4th and 6th PAAs; **C – C′**. 35s. The endothelium of the OFT, aortic sac, ventral aorta and the PAAs (numbered) are connected. Note that the endothelium (open arrowheads) is GFP^{+}; as – aortic sac; da – dorsal aorta; MIP – maximum intensity projection; OFT – outflow tract; va – ventral aorta. Numbers mark positions of the PAAs or pharyngeal arches. All scale bars are 100 μm.

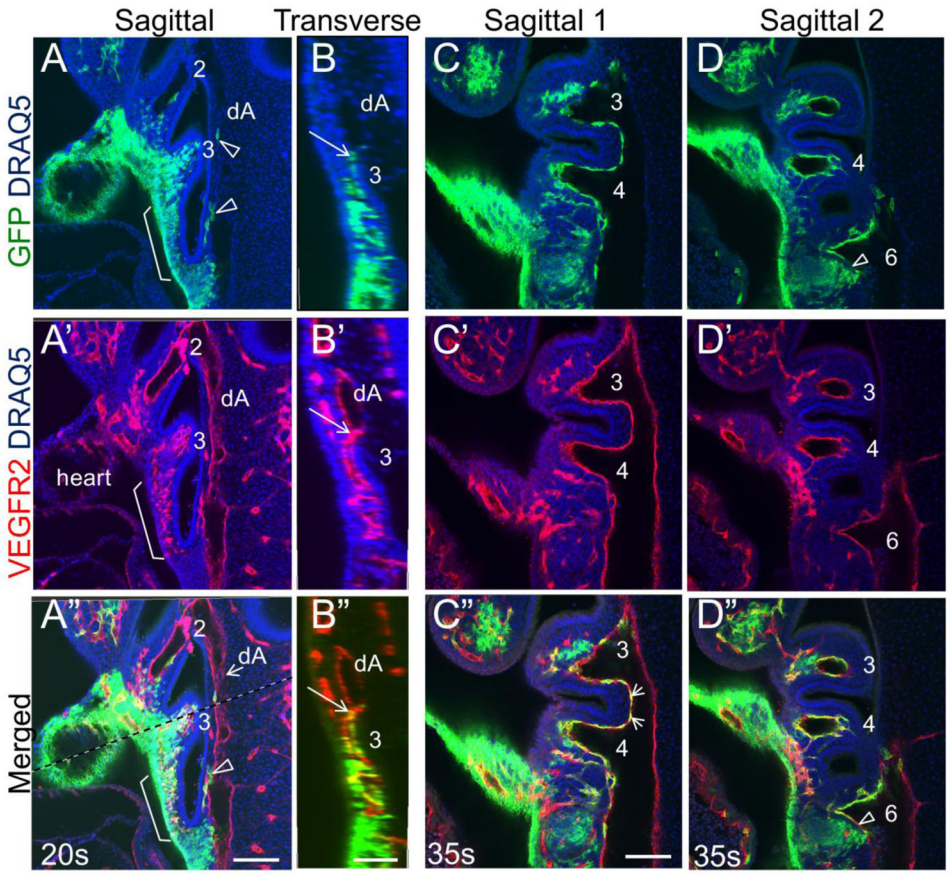

Figure 4. Junctions between the PAAs and the dorsal aorta contain GFP^{+} and GFP^{-} endothelial cells

All panels show optical sections through Mef2C-AHF-Cre; ROSA^{mTmG} embryos dissected at E9.0 (**A – B″**) or E10.5 (**C – D″**). **A – B″**. Sagittal optical section through E9.0, 20s embryo. PAAs are numbered. The endothelium in the 2nd PAA is mostly GFP^{-}. Pharyngeal plexus in the 3rd arch and in the region of the future 4th and 6th arches (bracket) is GFP^{+}; Open arrowheads point to GFP^{+} cells in the dorsal aorta (dA). Dashed line in **A″** marks the plane of transverse optical sections in **B – B″. B – B″**. Transverse optical sections through a GFP^{+} cell in the dorsal aorta show the connection between the dorsal aorta and the pharyngeal plexus, long arrows in **B – B″. C – D″**. Two optical sections through E10.5, 35s embryo. PAAs are numbered. **C – C″**. Ventral surface of the dorsal aorta adjacent to the PAAs contains GFP^{+} cells, arrows. **D – D″**. GFP^{-} cells are seen at the junction of the 6th PAA with the dorsal aorta (open arrowhead). Magnification is the same in **A – A″** and **C – D″** scale bars are 100 μm. Scale bars in **B – B″** are 50 μm.

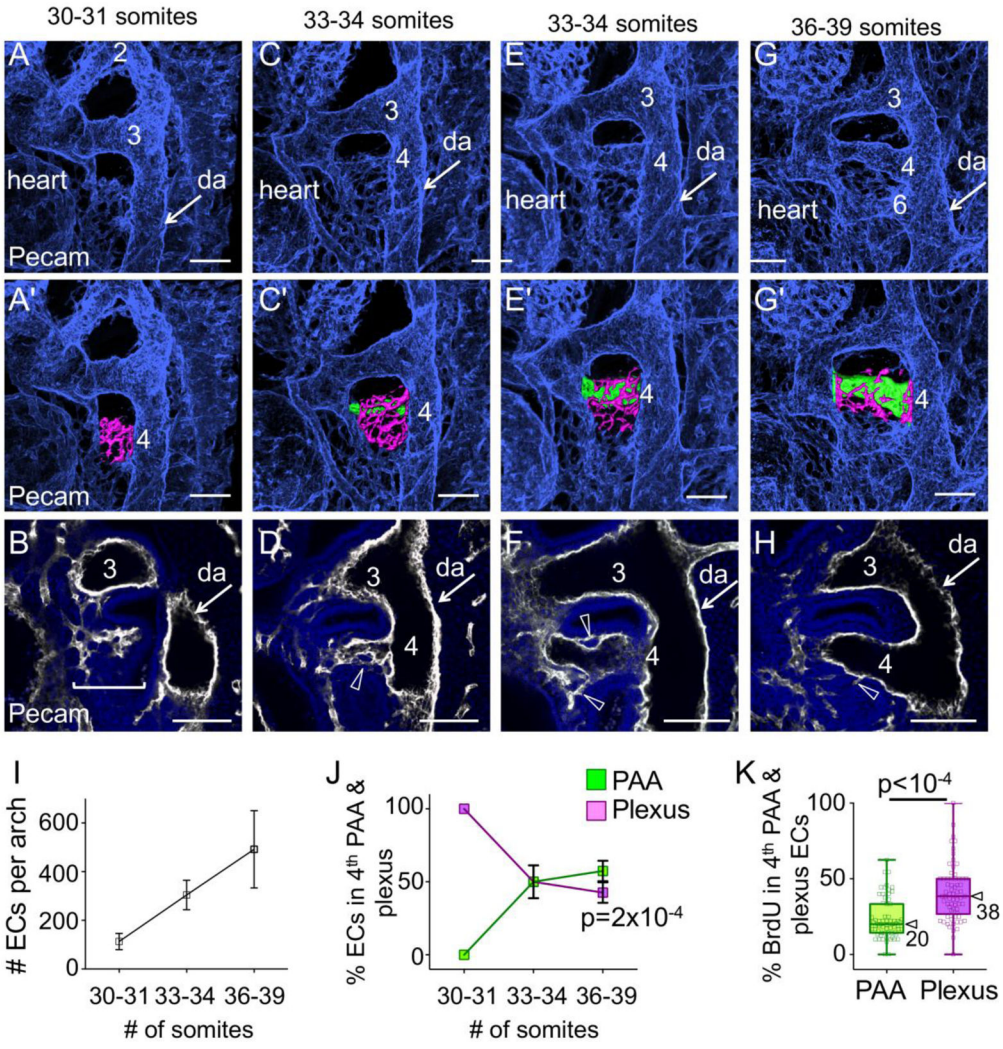

Figure 5. The 4th pair of PAA forms by the coalescence of plexus endothelial cells

Embryos at different somite stages were stained to detect Pecam1 and imaged by confocal immunofluorescence microscopy. **A, C, E, G**. 3D reconstructions (maximum intensity projections) of pharyngeal vasculature; one side of each embryo is shown in each panel. Pharyngeal arches are numbered, da – dorsal aorta. Endothelium in the 4th pharyngeal arch shown in **A, C, E,** and **G** was surface rendered in **A′, C′, E′,** and **G′** (see Methods and Sup. Fig. 1). Sagittal optical sections through the embryos in **A, C, E,** and **G** are shown in **B, D, F,** and **H. A, A′, B.** Only uniform endothelial plexus is present in the 4th arch at 30s–31s; it is surface rendered in pink in **A′** and underlined by a bracket in **B. C – F.** A slightly younger (**C – D**) and a slightly older (**E – F**) embryo with 33–34s are shown. A thin 4th PAA is visible at 33 – 34s. The PAA is surface rendered in green and the plexus is surface rendered in pink in **C′** and **E′**. Optical sagittal sections in **D** and **F** show the plexus endothelium (open arrowheads) connecting with the PAA. **G – H.** In the evening of E10.5, the 4th PAA is nearly completely formed (**G**), surface rendered green in **G′**. It has a large lumen (**H**) and fewer endothelial cells in the plexus than at 33–34s, rendered in pink in **G′**; arrowhead in **H**. Arrows point to the dorsal aorta. **I.** Growth of endothelial population in the 4th pharyngeal

arch. **J.** As the 4th PAA grows in size, the proportion of endothelial cells in the PAA increases (green line), while the proportion of endothelial cells in the plexus decreases (pink line). **K.** Proliferation index of plexus endothelial cells is nearly 2-fold higher than in the PAA. Box plots with all data points are shown, error bars span the minimum to maximum values. The box contains 50% of the data points and the horizontal bar inside the box marks the median. Unpaired, 2-tailed Student's t test was used to calculate p values. All scale bars are 100 μm.

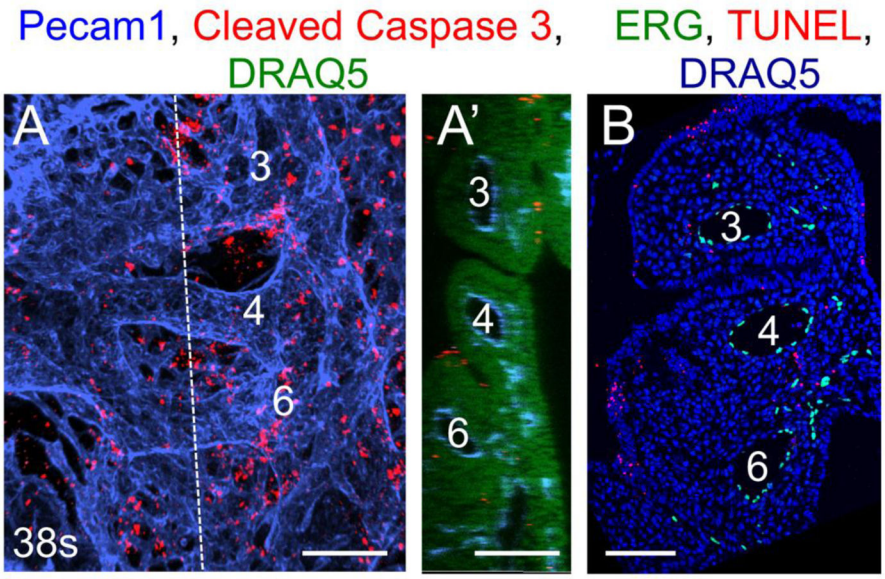

Figure 6. Survival of endothelial cells in the pharyngeal arches

A. 3D reconstruction of the entire pharyngeal region on one side of the embryo. Staining for cleaved caspase 3 **(A – A′)** shows minimal apoptosis in the pharyngeal arch endothelium; The dashed line marks the plane of optical section shown in **A′. B.** TUNEL assay using frozen sections through pharyngeal arches confirmed minimal apoptosis in the endothelium within the arches in E10.5 embryos. Scale bars are 100 μm.